metals

MDPI

Article

Selection of Strongly Basic Anion Exchangers for the Removal of Zn(II) and Pb(II) from Nickel Electrolytes: Functional Group, Matrix Structure, and Sorbent Stability

Elena Belogurova [1,2,*], Nikolai Tarasenko [1] and Alexandr Kasikov [1]

[1] Tananaev Institute of Chemistry—Subdivision of the Federal Research Centre "Kola Science Centre of the Russian Academy of Sciences", 26a Akademgorodok, 184209 Apatity, Russia; a.kasikov@ksc.ru (A.K.)
[2] Joint-Stock Company "Group of Companies "Rusredmet", 15/3A, Vosstanovleniya Street, 198320 Krasnoye Selo, Russia
* Correspondence: e.belogurova@rusredmet.ru

Abstract

Deep removal of zinc and lead from chloride nickel solutions is a key step in producing high-quality electrolytic nickel. This work compares five strongly basic anion exchangers for the sorption of Zn(II) and Pb(II) from a real nickel catholyte, focusing on the type of functional group (pyridinium vs. quaternary ammonium), the matrix structure (gel vs. macroporous), and the exchange capacity. The macroporous pyridinium anion exchanger AMP-p exhibits an increased affinity for large, easily polarizable $PbCl_n^{n-}$ complexes, reaching R(Pb) = 62.0%. The macroporous structure substantially improves the kinetics: AMP-p achieves 83.7% Zn removal within 15 min, whereas gel-type sorbents require 60–120 min. After three sorption–desorption cycles, the irreversible loss of functional groups was 22–30%. The protective effect of the macroporous matrix was selective and depended on the type of functional group: LSC688 (macroporous, quaternary ammonium) lost 27% of its FTIR signal, whereas AV-17-8 (gel, quaternary ammonium) lost 24%, so macroporosity alone does not guarantee higher stability. The loss of static exchange capacity was systematically lower than the FTIR-determined loss of functional groups (17.2–23.1% vs. 22–30%), indicating that part of the structural changes does not yet lead to complete deactivation of the ion-exchange sites. In dynamic tests at 70 °C, AMP-p provided a dynamic breakthrough capacity of 0.363 mmol/g for Zn and 99% Zn desorption. Based on the combination of functional stability, kinetics, and cycling resources, the macroporous pyridinium anion exchanger is recommended for the deep purification of chloride nickel solutions from Zn(II) and Pb(II).

Keywords: zinc; lead; ion-exchange resins; functional groups; chloride media; sorbent stability

Check for updates

Academic Editor: Petros E. Tsakiridis

Received: 28 October 2026
Revised: 23 November 2026
Accepted: 24 November 2026
Published: 27 November 2026

Copyright: © 2026 by the authors. Licensee MDPI, Basel, Switzerland. This article is an open access article distributed under the terms and conditions of the Creative Commons Attribution (CC BY) license.

1. Introduction

The removal of zinc and lead from chloride nickel solutions is an important task in hydrometallurgy, particularly in the processing of nickel–cobalt raw materials, leach solutions of sulfide concentrates, and spent sulfate–chloride electrolytes. The presence of zinc adversely affects the quality of cathode nickel: the standard electrode potential of Zn^{2+} ($E^\circ = -0.76$ V) is significantly more negative than that of Ni^{2+} ($E^\circ = -0.25$ V), so zinc is preferentially deposited on the cathode, causing zinc embrittlement of nickel, deterioration of the surface quality, and a decrease in current efficiency. As the demand for high-purity nickel grows, the requirements for the residual zinc concentration in the electrolyte become

increasingly stringent. Lead is also a harmful impurity: even small amounts of Pb in the electrolyte impair the structure of the nickel deposit and reduce its commercial grade.

Chloride systems have a number of features that distinguish them from sulfate systems: a high chloride concentration leads to the formation of stable metal chloride complexes, and the ionic strength of the solution and the activity of the components change, which substantially affects sorption processes. In chloride solutions, zinc exists predominantly as $ZnCl^+$, $ZnCl_2$, $ZnCl_3^-$, $ZnCl_4^{2-}$, complexes, the ratio of which depends on the chloride concentration and pH; similarly, $NiCl^+$ and $NiCl_2$ are formed for nickel. At elevated chloride concentrations typical of chloride nickel solutions, a significant fraction of zinc is present as anionic complexes, which opens the possibility of using anion-exchange resins for its selective recovery [1,2].

Both extraction and sorption schemes are used for the purification of chloride nickel solutions from zinc. The extraction method, used in particular in the purification of concentrated nickel solutions, is characterized by losses of the organic phase, complexity of the equipment, and fluctuations in the zinc content of the strip liquor [3,4]. The chloride solution chemistry underlying Zn and Pb separation is well documented in earlier reviews. Aprahamian and Demopoulos [5] reviewed the chloro-chemistry and solvent extraction behaviour of Zn and Pb (among other elements) in acid chloride media and established that most of these elements form anionic chloro-complexes at HCl concentrations > 1.0 M, extracting via ion-pair formation with strongly basic extractants (amines) as well as weaker ones (TBP, TOPO, 8-hydroxyquinoline). Jha et al. [6] subsequently reviewed solvent extraction of zinc from chloride solutions, covering acidic, basic, and solvating extractants, kinetics, mechanism, species formed in the organic phase, and stripping. More recently, Najafi et al. [7] demonstrated high selectivity for Zn(II) and Cd(II) over Ni(II) and Co(II) using commercial ionic liquids (Aliquat IL336, Cyphos IL101), with the metals extracted as anionic chloro-complexes via an anion-exchange mechanism. Membrane-based approaches have also been explored: Sarfraz et al. [8] reported selective transport of Zn^{2+} and Ni^{2+} through a supported liquid membrane with cyclohexylamine as carrier, with Zn^{2+} transported more efficiently than Ni^{2+} (87% vs. 72%). These studies confirm that extraction and membrane methods offer intrinsic selectivity for Zn over Ni in chloride media; however, they target model, adjacent, or PGM-refining systems rather than real nickel electrolyte and do not address simultaneous deep removal of Zn and Pb. Ion-exchange sorption, owing to the simplicity of the equipment, the absence of organic solvents, and its applicability to the deep removal of impurities from dilute solutions, is attracting increasing attention [9–11]. Recent sorption studies have further advanced this field. Cheng et al. [12] prepared an ionic-liquid composite anion-exchange resin and applied it to real nickel electrolyte, achieving 97.28% Zn removal and retaining >85% capacity after six regeneration cycles. Chen et al. [13] studied the thermodynamics and kinetics of Zn(II) sorption from chloride solutions on the DOWEX MSA-1 anion exchanger, and Barlık [14] optimized the sorption of zinc chloride complexes from acidic solutions on anionic resins. The specific problem of Pb and Zn removal from nickel electrolyte has also been recognized in earlier work: Chen et al. [15] discussed the behaviour of Pb and Zn during nickel electrolysis and compared chemical precipitation and ion exchange for their removal, while Zhu [16] reviewed purification methods for nickel solutions with respect to Fe, Cu, Zn, Ca, Mg, and Na. These works confirm the relevance of anion exchange for Zn removal from chloride media, but none of them systematically compares commercial strongly basic anion exchangers in terms of functional group type, matrix structure, and long-term stability under acidic chloride conditions at elevated temperature. However, the efficiency of an ion-exchange resin is not determined solely by its classification as a “strongly basic anion exchanger”: the nature of the functional group, the

physical structure of the polymer matrix, and the exchange capacity jointly determine the selectivity, kinetics, and stability of the sorbent in a specific medium [1].

Strongly basic anion exchangers, chelating resins (IDA, aminophosphonate), inorganic sorbents, and biosorbents are used for zinc recovery from solutions. Chelating resins provide high selectivity toward zinc in the presence of nickel owing to differences in the stability constants of the complexes; however, their efficiency depends substantially on pH and decreases in acidic media typical of nickel electrolytes; the same limitation applies to hydrated oxides, zeolites, and chitosan [17–19]. Under these conditions, the advantage is retained by strongly basic anion exchangers that sorb anionic zinc chloride complexes; as the chloride concentration increases, the fraction of $ZnCl_3^-$ and $ZnCl_4^{2-}$ increases, which raises the sorption capacity, but at the same time the uptake of nickel as $NiCl_3^-$ becomes possible, reducing the selectivity [1,2,20].

In chloride nickel solutions, zinc sorption can proceed via ion-exchange, complexation, and physical adsorption mechanisms; in the case of anion exchangers, ion exchange of anionic chloride complexes dominates, and the selectivity is determined by the ratio of the stability constants of the metal complexes with the functional groups of the sorbent and with chloride ions in solution [1,21]. The process efficiency is substantially affected by the chloride concentration (optimum usually 100–250 g/L), pH (1–3 for anion exchangers), temperature (20–60 °C), competition from nickel, and the contact time, which depends on the kinetic characteristics of the sorbent [1,2,22]. It has been shown that macroporous anion exchangers have better wear resistance and mechanical strength than gel-type analogues, as well as a higher dynamic breakthrough capacity in the removal of zinc from nickel electrolyte [2]. For the deep purification of chloride nickel solutions from zinc, column schemes with an anion-exchange resin operating at pH $\leq$ 6.0 and a temperature of 30–70 °C have been proposed [23].

Depending on the volume of solutions to be processed, periodic and continuous sorption schemes are used. In industrial conditions, columns with a fixed bed of sorbent or countercurrent apparatuses are more often used, allowing more complete recovery and a reduction in sorbent consumption [5,6,24]. For the desorption of zinc from chelating resins, sulfuric or hydrochloric acid solutions (1–2 M) are usually used, and for anion exchangers, ammonia or sodium hydroxide solutions; in this case, it is important to ensure complete desorption and preservation of the resin capacity during repeated use [1,21,22]. An alternative approach is the desorption of zinc from the anion exchanger with water, based on the destruction of the chloride complex upon dilution, which reduces reagent consumption and simplifies the regeneration scheme [20].

Although anion exchange is known to be effective for zinc removal from chloride solutions, most reported studies evaluate only the sorption capacity in the first cycle and do not consider the stability of the ion exchanger as an independent selection criterion. Meanwhile, it is precisely the stability of the functional groups and the matrix in an acidic chloride medium at elevated temperature that determines the industrial applicability of a sorbent [22,25–28]. However, the combined effect of the functional group type and the matrix structure on the simultaneous removal of Zn(II) and Pb(II) from real nickel catholyte has not been systematically compared. This gap is particularly important for industrial practice, where the service life of the sorbent and its ability to operate at the process temperature (60–70 °C) directly determine the economics of the purification step.

The aim of this work was to select the optimal anion exchanger for the purification of chloride nickel solution from zinc and associated lead based on the combination of sorption and operational characteristics. Particular emphasis is placed on the stability of the functional groups and the matrix under conditions close to industrial operation, since it is this parameter that ultimately determines the sorbent service life.

2. Materials and Methods

2.1. Characterization of Sorbents

Five industrial strongly basic anion exchangers were used in this work: AMP-p (OOO GP "Smoly", Moscow, Russia), AV-17-8 (OOO PO "TOKEM", Kemerovo, Russia), and Seplite® LSC662, LSC688, and SA6700 Cl (Sunresin, Xi'an, China). Structurally, AMP-p and LSC662 are based on 1-methylpyridinium chloride functional groups (-$[C_5H_5N(CH_3)Cl]^-$), whereas AV-17-8, LSC688, and SA6700 Cl are based on benzyltrimethylammonium chloride groups (-CH_2-$N^+(CH_3)_3Cl^-$). All sorbents utilize styrene-divinylbenzene (St-DVB) copolymer matrices.

The main characteristics of the sorbents are given in Table 1. The strategy for selecting the sorbents was designed to enable an independent assessment of the influence of three key variables: the type of functional group—pyridinium (AMP-p, LSC662) or quaternary ammonium (AV-17-8, LSC688, SA6700); the matrix structure—macroporous (AMP-p, LSC688) or gel (AV-17-8, LSC662, SA6700); and the exchange capacity—in the range from ≥1.2 to ≥1.4 meq/mL. Such an experimental design allows the observed differences in sorption characteristics to be attributed to the influence of specific structural parameters—the type of functional group, the matrix structure, and the exchange capacity—considering each of them as an independent variable.

Table 1. Physicochemical characteristics of the studied anion exchangers.

Sorbent	AMP-p	AV-17-8	LSC662	LSC688	SA6700 Cl
Matrix structure	Macroporous	Gel	Gel	Macroporous	Gel
Functional group	1-methylpyridinium	Benzyltrimethylammonium (type 1)	1-methylpyridinium	Benzyltrimethylammonium (type 1)	Benzyltrimethylammonium (type 1)
Size (mm)	0.5–1.2	0.4–1.25	0.8–2.0	0.7–2.0	0.55 ± 0.05
SEC (meq/g)	≥1.3	≥1.2	≥1.3	≥1.2	≥1.4
Feature	Analogue of LSC662	Analogue of LSC688/SA6700	Analogue of AMP-p	Analogue of AV-17-8 (macroporous)	Monodisperse, CU ≤ 1.1

At the molecular level, the superior affinity of pyridinium groups toward large, polarizable $PbCl_n^{n-}$ anions is attributed to the delocalization of the positive charge within the aromatic ring, which facilitates strong ion-pair interactions and additional polarization effects. In contrast, the charge in quaternary ammonium groups is localized, resulting in predominantly electrostatic interactions. The SA6700 sorbent is characterized by a monodisperse particle-size distribution (0.55 ± 0.05 mm, coefficient of uniformity ≤ 1.1), which provides low hydraulic resistance and uniform flow distribution in column apparatuses; at the same time, the gel structure of the matrix causes increased internal diffusion resistance, which may limit the sorption kinetics.

2.2. Experimental Procedure

Static experiments were carried out on a real nickel catholyte solution after the copper removal stage (pH = 1.5; C(Zn) = 0.62 mg/L; C(Pb) = 2.21 mg/L), which represents a complex sulfate-chloride system with a high sulfate ion content (~60 g/L) [10]. The presence of sulfate ions in combination with chloride ions creates a strong salting-out effect, promoting the formation and stabilization of anionic zinc chloride complexes and enhancing the efficiency of anion-exchange sorption. The use of a real nickel catholyte rather than a model solution ensures that the observed sorption behavior accounts for the combined

effects of sulfate, chloride, and competing metal ions present in the industrial stream. The influence of temperature (20, 40, 60 °C), solid-to-liquid ratio (S:L = 1:10–1:100), and contact time (15–120 min) was studied. Desorption was carried out with a 3% H_2SO_4 solution at 40 °C, S:L = 1:10, for 2 h; the choice of eluent is due to the ability of sulfuric acid to form stable complexes with Zn^{2+} and Pb^{2+} and to provide sufficient acidity (pH ≈ 2–2.5) to break the ion-exchange bonds without significant degradation of the polymer matrix [21].

To assess the chemical stability of the anion exchangers, an accelerated (stress) testing method was used: three successive sorption–desorption cycles were performed. Sorption was carried out under increased loads (80 ± 1 °C, 24 h, S:L = 1:25), and desorption was performed with 10 g/L H_2SO_4 at 40 ± 1 °C for 2 h (S:L = 1:10). The choice of more severe conditions (80 °C and 24 h) compared with the operating conditions (60–70 °C) is due to the need to intensify hydrolytic degradation processes in order to obtain reliable data on the service life of the sorbent within a limited number of cycles (3). The state of the functional groups was monitored by Fourier-transform infrared spectroscopy (4000–400 cm^{-1}, KBr pellets). The relative intensity of the characteristic bands (1630 cm^{-1} for pyridinium groups, 1200–1250 cm^{-1} for quaternary ammonium groups) was calculated as the ratio of the peak area/height to the corresponding value in the initial sample after normalization to an internal standard (the band at ~800 cm^{-1} for pyridinium and ~1600 cm^{-1} for quaternary ammonium sorbents), which makes it possible to identify changes in the ionogenic groups, signs of oxidative degradation of the polymer chain (C=O bands at ~1720 cm^{-1}), and to evaluate irreversible degradation, as well as to separate reversible physical effects from irreversible chemical degradation [25]. In addition, the static exchange capacity (SEC) of the initial and spent samples was determined according to DIN 54402:2009-04 [27].

2.3. Dynamic Column Tests

Dynamic tests were carried out on a laboratory setup (a polypropylene sorption column with a jacket, an internal diameter of 2.3 cm, and a height of 50 cm; a peristaltic pump; a sampling system) using the AMP-p sorbent (Figure 1). The tests were carried out at 70 ± 1 °C, which simulates the solution temperature in an industrial column.

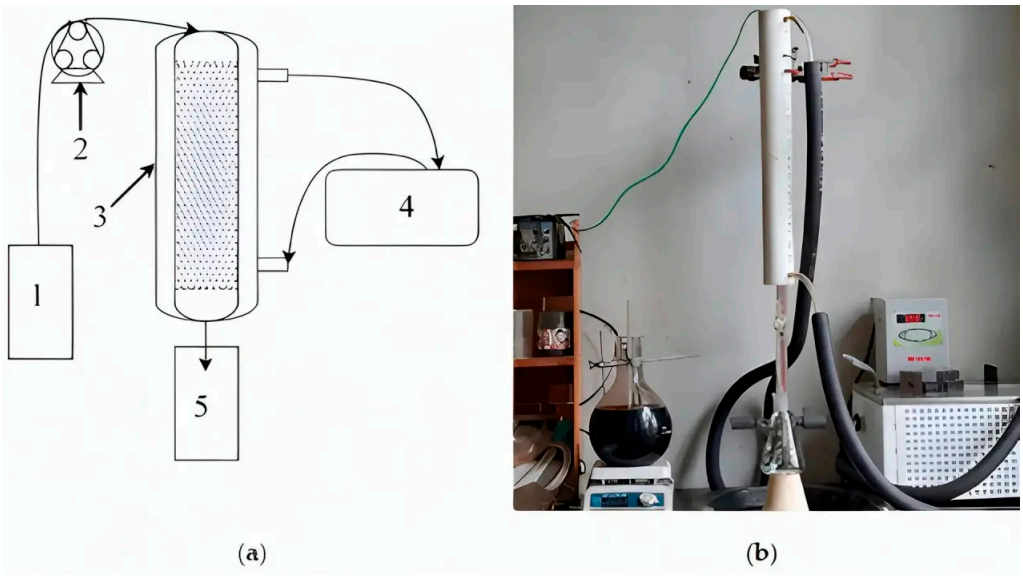


Figure 1. Laboratory setup for dynamic tests: (**a**) schematic diagram—1, feed solution tank; 2, peristaltic pump; 3, jacketed sorption column; 4, circulating thermostat; 5, effluent collector; (**b**) photograph of the actual laboratory setup.

The volume of the swollen sorbent was 100 mL (bed height 24 cm), the mass of the air-dry sorbent was 67 g, and the free volume of the column was 0.038 L (0.38 bed volumes). The zinc concentration in the laboratory solution was increased to 490 mg/L by adding $ZnCl_2$ for reliable analytical control and to obtain the dynamic breakthrough capacity (DBC) as a universal characteristic recalculated to the real solution. Test conditions: temperature 70 ± 1 °C; pH = 1.5; $C_0(Zn)$ = 490 mg/L; $C_0(Pb)$ = 1.1 mg/L; feed rate 5 mL/min (contact time 20 min); the feed was passed until V = 5.2 L ($C/C_0 \approx 0.10$ for Zn); the run was terminated before complete saturation of the bed was reached.

The dynamic exchange capacity was calculated by the formula:

$$DBC = \frac{(C_0 - 0.1C_0)\cdot V_{breakthrought(corr.)}}{m_{sorb}}, \quad (1)$$

where C_0 is the metal concentration in the feed; $0.1C_0$ is the breakthrough concentration corresponding to $C/C_0 = 0.1$ (10% of the initial); $V_{breakthrough(corr.)} = V_{breakthrough(exp.)} - V_{free}$ is the volume of solution passed to the breakthrough point, corrected for the free volume of the column, L; m_{sorb} is the mass of the air-dry sorbent, g.

The total dynamic capacity (TDC) was calculated by trapezoidal integration of the experimental breakthrough curve over the measured points up to the end of the run ($C/C_0 \approx 0.10$ at 5.2 L; Supplementary Table S1):

$$TDC = \frac{m_0}{m_{sorb}} \int (1 - C/C_0) dV. \quad (2)$$

Because the bed was not fully saturated at the end of the run, the integrated TDC represents the amount retained over the run rather than the absolute saturation capacity. For Pb, the integral was not used for capacity calculation, since the Pb loading is close to the analytical detection limit; the retained Pb amount is discussed in Section 3.6.

To recalculate the volume of the laboratory experiment to the volume of the real industrial solution, Equation (3) was used:

$$V_{real}(L/g) = \frac{DBC\ (mmol/g)}{C_{real}(mmol/L)} \quad (3)$$

where C_{real} is the Zn concentration in the real industrial solution (0.62 mg/L = 9.48×10^{-3} mmol/L).

After sorption, the column was washed with distilled water at 70 °C (5 mL/min, 250 mL) until chloride ions were absent and C(Zn) < 0.1 mg/L. Desorption of zinc and lead was carried out with a 10% H_2SO_4 solution at 40 °C at a rate of 2 mL/min; the eluent volume was 550 mL, and fractions of 75 mL were collected; the completion criterion was C(Zn) in the eluate < 0.5 g/L.

The determination of metals in the samples was carried out using the atomic absorption spectrometer "HGA" 4100 ZL (Perkin Elmer, Shelton, CT, USA), emission spectrometer ICPS-9000 (Shimadzu, Kyoto, Japan) and mass spectrometer ELAN 9000 DRC-e (PerkinElmer, Shelton, CT, USA).

3. Results and Discussion

3.1. Influence of the Functional Group on Selectivity

To assess the contribution of the type of functional group to the efficiency of zinc and lead recovery, a comparative study of five strongly basic anion exchangers was carried out under identical conditions (Table 2). The effect of the functional group is best isolated by comparing sorbents with the same matrix. AMP-p (pyridinium, macroporous) gives R(Pb) = 62.0% (β = 0.76), whereas LSC688 (quaternary ammonium, macroporous) gives R(Pb) = 26.7% (β = 0.31); with the matrix held constant, the pyridinium group clearly

provides higher Pb affinity. However, the gel pyridinium resin LSC662 gives β = 0.29, which is lower than that of the quaternary ammonium resins (β = 0.31–0.43). This shows that the matrix must be accessible for the pyridinium group to express its affinity: in the gel matrix, diffusion limitations prevent the pyridinium group from realizing its intrinsic selectivity. We also note that β = R(Pb)/R(Zn) depends on both R(Pb) and R(Zn), and the high R(Zn) of LSC662 (86.1%) lowers its β even when R(Pb) is moderate; the pair AMP-p/LSC688 therefore provides a more direct comparison of Pb affinity. The value β = R(Pb)/R(Zn) characterizes the selectivity of the sorbent toward lead in the presence of zinc: the higher β, the higher the affinity for Pb.

Table 2. Comparative efficiency of Zn and Pb recovery by the studied sorbents. Conditions: T = 40 °C, S:L = 1:50, τ = 2 h.

Sorbent	Functional Group	Matrix	R(Zn), %	R(Pb), %	β = R(Pb)/R(Zn)
AMP-p	Pyridinium	Macroporous	81.5	62.0	0.76
AV-17-8	Quaternary ammonium	Gel	80.2	34.8	0.43
LSC662	Pyridinium	Gel	86.1	24.9	0.29
LSC688	Quaternary ammonium	Macroporous	85.6	26.7	0.31
SA6700 Cl	Quaternary ammonium	Gel	84.7	28.5	0.34

All sorbents demonstrate high degrees of Zn(II) recovery (80–86%), with the difference between them not exceeding 6%. This means that in the sulfate–chloride nickel electrolyte with a high background content of chloride ions (30–60 g/L) and sulfate ions (≈60 g/L), zinc is present in the form of anionic chloride complexes ($ZnCl_3^-$, $ZnCl_4^{2-}$). Sulfate ions act as an additional salting-out agent, reducing the solubility of the chloride complexes and promoting their transfer into the ion exchanger phase, where they are effectively captured by any strongly basic anion exchanger. Under single-contact conditions, therefore, the exchange capacity is not the limiting factor for Zn uptake.

The influence of the type of functional group on Pb(II) sorption is much more pronounced, and its effect is best isolated when the matrix structure is held constant. With the same macroporous matrix, the pyridinium resin AMP-p gives R(Pb) = 62.0% (β = 0.76), whereas the quaternary ammonium resin LSC688 gives R(Pb) = 26.7% (β = 0.31), i.e., the pyridinium group clearly provides a higher Pb affinity. The comparison of the two pyridinium sorbents, AMP-p (macroporous) and LSC662 (gel-type), shows in turn that the matrix must be accessible for the pyridinium group to express its affinity: the gel-type pyridinium resin gives R(Pb) = 24.9%, which is lower than that of all quaternary ammonium sorbents (β = 0.31–0.43), so diffusion limitations in the gel matrix prevent the pyridinium group from realizing its intrinsic selectivity. We also note that β = R(Pb)/R(Zn) depends on both R(Pb) and R(Zn): the high R(Zn) of LSC662 (86.1%) lowers its β even when R(Pb) is moderate, so the AMP-p/LSC688 pair with an identical matrix provides the more direct comparison of Pb affinity.

The pronounced affinity of pyridinium groups for Pb observed here is consistent with the established chloro-chemistry of Pb in chloride media, where Pb(II) forms anionic complexes that extract or sorb via ion-pair/anion-exchange mechanisms [5]. In the macroporous pyridinium resin AMP-p, R(Pb) reached 62.0%, whereas the gel-type pyridinium LSC662 gave only 24.9%, despite nominally the same functional group. This supports the view that in concentrated chloride media the accessibility of the matrix, rather than the intrinsic exchange capacity alone, can become the limiting factor for bulky Pb chloro-anions, in line with the matrix effects reported for Zn chloride complex sorption on strongly basic resins [16,17].

The size of the chloro-complexes provides an additional explanation for the observed selectivity pattern. In concentrated chloride media, Zn(II) is present mainly as the tetrahedral $[ZnCl_4]^{2-}$ complex (ionic radius of Zn^{2+} ≈ 0.74 Å for CN = 4), whereas Pb(II) forms a series of octahedral complexes $PbCl_n^{n-2}$ (n = 3–6) with a significantly larger ionic radius of Pb^{2+} (≈1.19 Å for CN = 6). The larger size and higher polarizability of the Pb chloro-complexes make the steric accessibility of the exchange sites more critical for Pb than for Zn. This is consistent with the much stronger effect of the matrix structure on Pb sorption (AMP-p 62.0% vs. LSC662 24.9%) than on Zn sorption (80–86% for all sorbents): the bulky $PbCl_4^{2-}$ anions can only access the internal exchange sites of the macroporous matrix, whereas the smaller $[ZnCl_4]^{2-}$ complex diffuses readily into both gel-type and macroporous resins. The higher polarizability of $PbCl_4^{2-}$ also favors additional interaction with the aromatic pyridinium ring, which is reflected in the higher Pb/Zn selectivity of AMP-p ($\beta = 0.76$) compared with the quaternary ammonium sorbents ($\beta = 0.31$–0.43).

From a practical standpoint, this means that for nickel electrolytes containing both Zn and Pb, the choice of a pyridinium anion exchanger provides simultaneous removal of both impurities, whereas quaternary ammonium sorbents are effective mainly for Zn and leave a significant fraction of Pb in solution.

3.2. Influence of the Matrix Structure on Kinetics

To assess the influence of the polymer matrix structure on the rate of establishment of sorption equilibrium, a kinetic study of Zn(II) sorption by the studied anion exchangers was carried out at S:L = 1:50. The results are given in Table 3.

Table 3. Kinetics of Zn sorption. Conditions: S:L = 1:50.

Sorbent	Matrix	T, °C	R(Zn), % (15 min)	R(Zn), % (60 min)	R(Zn), % (120 min)
AMP-p	Macroporous	40	83.7	84.4	85.5
AV-17-8	Gel	40	56.2	84.0	85.6
LSC662	Gel	60	-	53.2	74.2
LSC688	Macroporous	60	-	54.8	72.6
SA6700 Cl	Gel	60	-	51.6	51.6

The kinetic advantage of the macroporous structure is evidenced not by a direct temperature-matched comparison across all samples (which is complicated by the intrinsic diffusion limitations of gel resins at lower temperatures), but by the fact that macroporous resins achieve high recovery rates under conditions where gel-type resins exhibit severe kinetic hindrance. As shown in Table 3, the macroporous pyridinium sorbent AMP-p at 40 °C already achieves 83.7% Zn recovery within 15 min and practically reaches equilibrium by 60 min. In contrast, the gel-type quaternary ammonium sorbent AV-17-8 at the same temperature (40 °C) extracts only 56.2% within 15 min and approaches equilibrium only by 60 min.

For the gel-type LSC662, the degree of recovery at 60 min is only 53.2% even at an elevated temperature of 60 °C. This temperature increase was necessitated by the intrinsic diffusion limitations of the gel matrix: at 40 °C, the LSC662 resin fails to establish equilibrium within the practical timeframe (reaching only 53.2% at 60 min). In contrast, the macroporous AMP-p achieves 84.4% recovery at 60 min under milder conditions (40 °C). Therefore, the kinetic advantage of the macroporous structure is evidenced not by a direct temperature-matched comparison but by the fact that macroporous resins achieve high recovery rates under conditions where gel-type resins exhibit severe kinetic hindrance and require higher temperatures to initiate diffusion.

The data for LSC688 (macroporous, 60 °C) and SA6700 (gel, 60 °C) further support this trend: despite the 20 °C temperature advantage, the macroporous LSC688 (54.8% at 60 min) only even marginally outperforms the gel-type SA6700 (51.6% at 60 min), indicating that for quaternary ammonium groups the chemical nature of the fixed ion may be a more limiting factor for kinetics than the matrix structure alone.

The exchange sites of gel-type resins are accessible only through the interchain spaces of the swollen polymer, which creates significant diffusion resistance, especially for large $PbCl_n^{n-}$ complexes. Despite the most uniform particle-size distribution, SA6700, because of its gel matrix, does not reach equilibrium within 120 min, which shows that particle-size uniformity does not compensate for the internal diffusion limitations of the gel structure.

The data obtained show that macroporous sorbents provide a high degree of zinc recovery within 15–30 min, whereas gel-type sorbents require 60–120 min. Under static conditions, all sorbents, including SA6700 with the highest SEC (≥1.4 meq/g), showed comparable degrees of Zn recovery (80–86%). This means that under single-contact conditions, the exchange capacity is not the limiting factor—the determining role is played by the functional group and the matrix structure.

For industrial column operation, this difference translates directly into the required contact time and, consequently, into the sorbent inventory and column size: the macroporous sorbent allows the contact time to be reduced to 15–30 min without loss of Zn removal efficiency, which is important for the purification of large volumes of nickel electrolyte.

3.3. Influence of Temperature

To assess the influence of temperature on the efficiency of Zn(II) and Pb(II) recovery, sorption on five anion exchangers was studied in the range of 20–60 °C at S:L = 1:50 and a contact time of 2 h. The obtained recovery values are shown in Figure 2 (a—Zn, b—Pb).

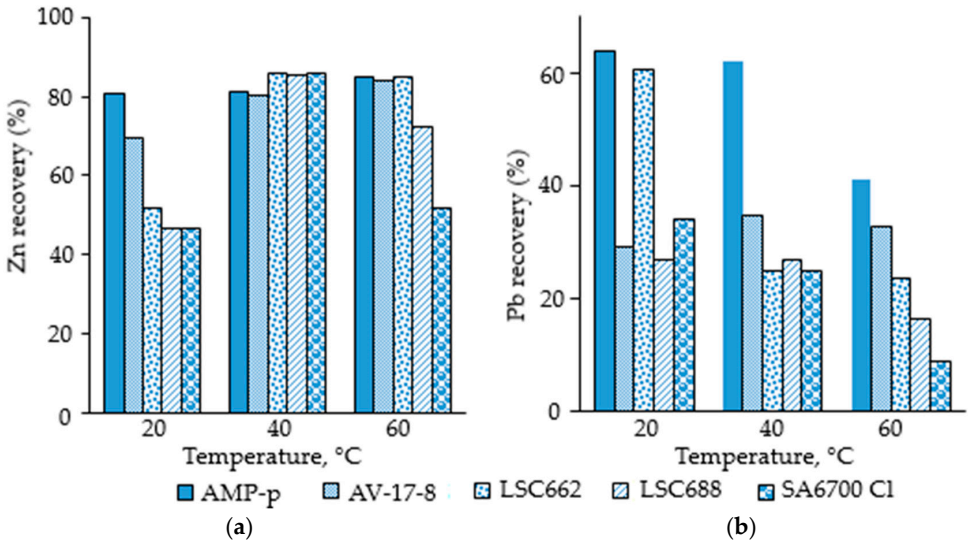


Figure 2. Influence of temperature on the degree of Zn (**a**) and Pb (**b**) recovery. Conditions: S:L = 1:50, τ = 2 h.

For zinc, an increase in temperature leads to an increase in the degree of recovery; the exceptions are LSC688 and SA6700 at 60 °C, where a noticeable decrease is observed (from 85.6% to 72.6% and from 86.1% to 51.6%, respectively), which is associated with the degradation of functional groups. The pronounced drop in Zn recovery for LSC688 (from 85.6% to 72.6%) and SA6700 (from 86.1% to 51.6%) at 60 °C, contrasted with the stability of AMP-p (83.7% at 40 °C vs. 85.5% at 60 °C in Table 3), further supports the conclusion that the macroporous pyridinium system possesses a unique combination of chemical and

structural robustness, whereas the gel-type quaternary ammonium sorbents are highly susceptible to thermally accelerated hydrolysis. For LSC662 at 60 °C, a slight decrease is also observed (from 86.1% to 85.0%), but within limits that do not affect the general trend. For lead, an increase in temperature above 40 °C leads to a decrease in the degree of recovery for all sorbents.

The influence of temperature is explained by differences in the stability of the functional groups and the matrix structure:

(1) Macroporous pyridinium sorbent: the macroporous structure provides fast diffusion and resistance to thermal hydrolysis; the pyridinium ring has increased stability in acidic chloride media owing to its aromatic nature.
(2) Gel-type pyridinium sorbent: the gel matrix creates additional diffusion limitations that require heating for activation. However, the same gel structure, in combination with the acidic medium and chloride ions at 60 °C, initiates hydrolytic cleavage of the pyridinium groups.
(3) Quaternary ammonium sorbents: degradation at 60 °C is associated with the known mechanism of hydrolytic decomposition of quaternary ammonium bases in an acidic medium with the formation of tertiary amines and alcohols. This degradation is most pronounced in the monodisperse gel-type sorbent, which may be due to its structure creating a higher local concentration of degradation products near the functional groups.

Since industrial nickel electrolyte is processed at 60–70 °C, the ability of the sorbent to maintain its capacity at elevated temperature without degradation is a critical selection criterion. The macroporous pyridinium sorbent retains its sorption performance at 60 °C, whereas the gel-type quaternary ammonium sorbents show a pronounced drop in Zn recovery, which is attributed to hydrolytic degradation of the functional groups.

3.4. Influence of S:L Ratio

To assess the influence of the solid-to-liquid ratio on the sorption efficiency, the recovery of Zn(II) and Pb(II) was studied at S:L ratios varying from 1:10 to 1:100. The obtained recovery values are shown in Figure 3 (a—Zn, b—Pb).

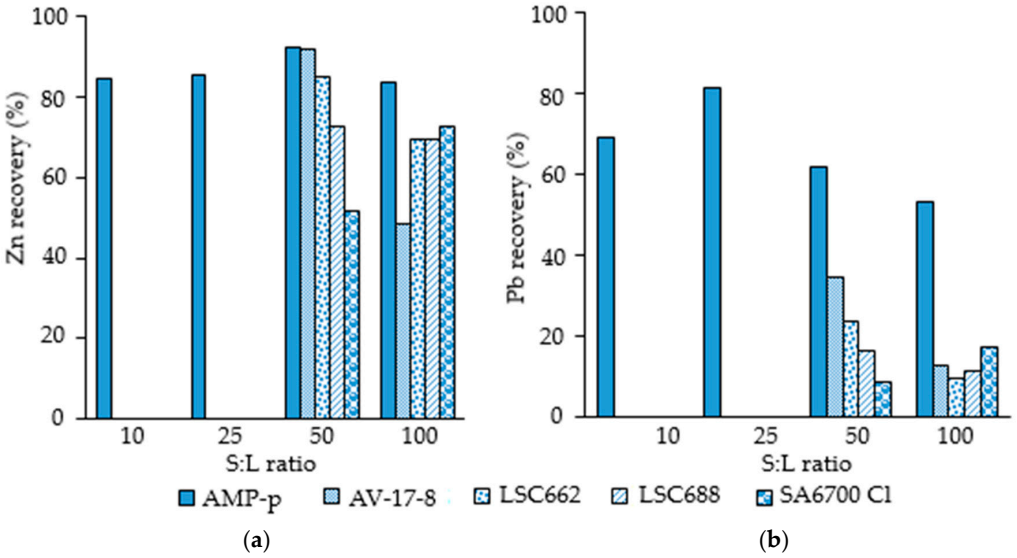


Figure 3. Influence of S:L on the degree of Zn (**a**) and Pb (**b**) recovery. Conditions: T = 60 °C, τ = 2 h.

The macroporous pyridinium sorbent demonstrates the highest stability to changes in S:L: the degree of zinc recovery remains at 83.5–92.6% over the entire range from 1:10

to 1:100. Gel-type sorbents are sensitive to an increase in S:L: upon transition from 1:50 to 1:100, the efficiency decreases sharply—for example, for AV-17-8 from 92.1% to 48.4% and for LSC662 from 85.0% to 69.4%.

3.5. Cyclic Stability: Degradation of Functional Groups and SEC Losses

To assess the stability of the anion exchangers to repeated use under aggressive conditions, three successive sorption-desorption cycles were carried out. The state of the functional groups was monitored by FTIR, and the change in ion-exchange properties was evaluated by the static exchange capacity (SEC). The obtained loss values according to FTIR and SEC are shown in Figures 4 and 5 and in Table 4.

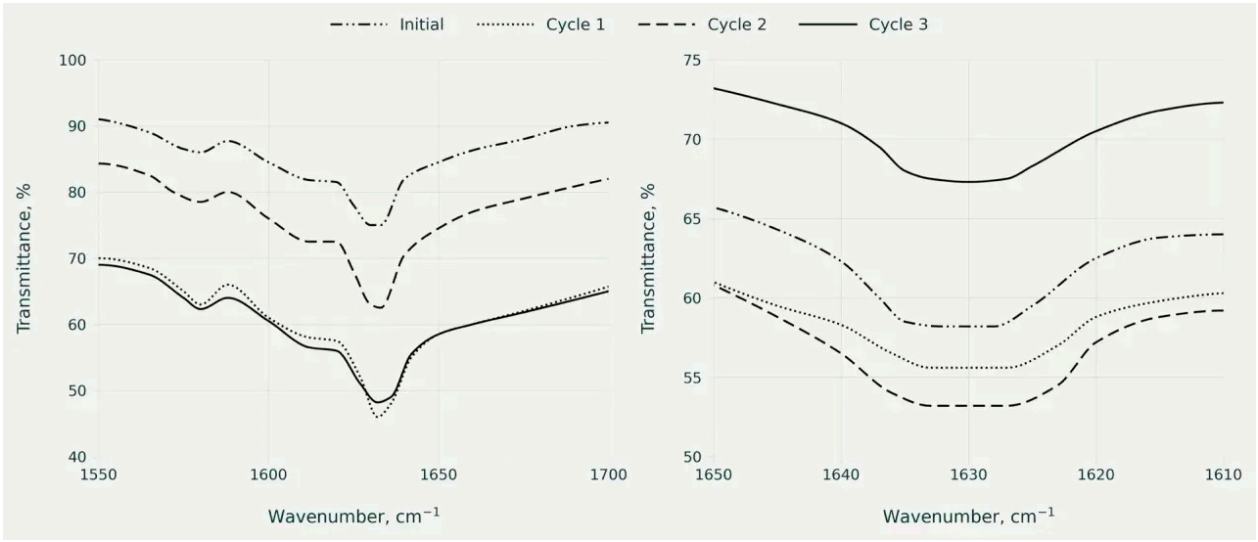


Figure 4. Relative intensity of the ν(C=N$^+$) band at 1630 cm^{-1} for pyridinium anion exchangers after 0, 1, 2, and 3 sorption-desorption cycles: (**a**) macroporous AMP-p; (**b**) gel-type LSC662. Band loss after 3 cycles: 22% and 29%, respectively.

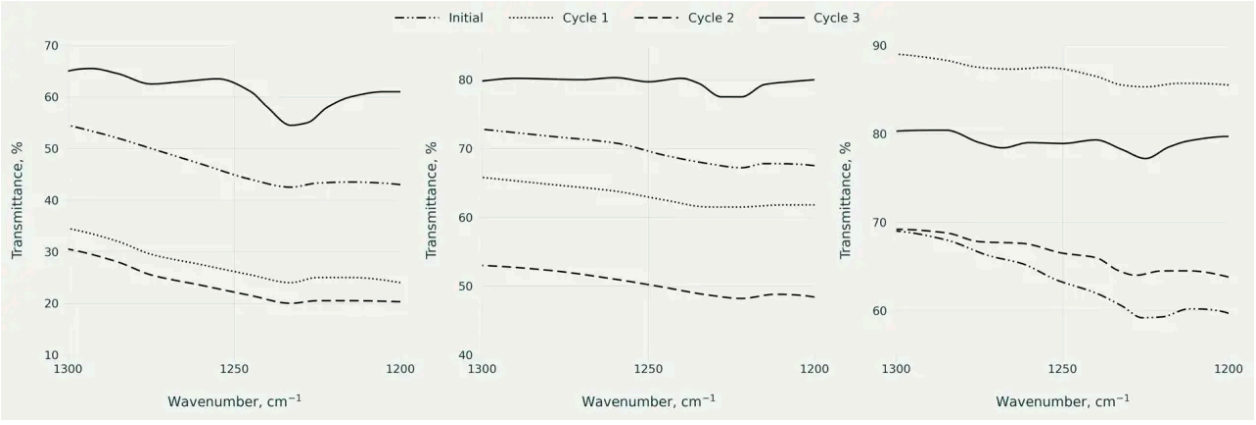


Figure 5. Relative intensity of the νas(C-N) band at 1200–1250 cm^{-1} for quaternary ammonium anion exchangers after 0, 1, 2, and 3 cycles: (**a**) gel-type AV-17-8; (**b**) macroporous LSC688; (**c**) monodisperse gel-type SA6700. Losses after 3 cycles: 24%, 27%, and 30%, respectively.

Table 4. Losses of functional groups (FTIR) and SEC after three cycles.

Sorbent	Functional Group	Key FTIR Band, cm^{-1}	FTIR Loss, %	SEC Loss, %	Delta, %
AMP-p	Pyridinium	1630 ($C=N^+$)	22	17.3	4.7
AV-17-8	Quaternary ammonium	1200–1250 (C–N)	24	17.2	6.8
LSC662	Pyridinium	1630 ($C=N^+$)	29	23.1	5.9
LSC688	Quaternary ammonium	1200–1250 (C–N)	27	19.6	7.4
SA6700 Cl	Quaternary ammonium	1200–1250 (C–N)	30	22.1	7.9

Three key observations regarding the chemical stability deserve discussion.

First, the nature of the degradation process. Across all five sorbents, no C=O band at 1720 cm^{-1} was detected in the FTIR spectra after three cycles. This indicates that oxidation via carbonyl-containing products is not the dominant pathway under the tested conditions. However, the absence of a C=O band does not exclude oxidation via other routes (e.g., radical pathways or ring oxidation without carbonyl formation), and the FTIR data alone cannot distinguish between acid-catalyzed hydrolysis and oxidation. The accelerated test conditions (80 °C, acidic medium, 24 h) are favorable for both pathways. Therefore, the degradation mechanism is presented here as a hypothesis—acid-catalyzed hydrolytic cleavage of the functional groups—rather than as a proven pathway. The systematic discrepancy between the FTIR-determined loss of functional groups (22–30%) and the loss of static exchange capacity (SEC, 17.2–23.1%), as shown in Table 4, indicates that a significant fraction of the structural changes detected by FTIR (e.g., local conformational stress or partial dealkylation of the nitrogen center) does not lead to complete deactivation of the ion-exchange site. Thus, while the chemical environment of the group changes, the site largely retains its accessibility for $ZnCl_4^{2-}$ anions. This functional preservation indicates that the observed spectral changes do not correspond to a total irreversible loss of the resin's working capacity.

Second, the protective effect of the macroporous matrix is selective and depends on the functional group type. For pyridinium resins, the macroporous AMP-p indeed shows lower degradation (22%) compared to the gel-type LSC662 (29%). The macroporous network facilitates more uniform ion and heat transport, reducing localized acid concentration gradients and thermal stress near the functional groups [25]. However, this protective effect is not universal. Among quaternary ammonium resins, the macroporous LSC688 (27%) shows greater FTIR loss than the gel-type AV-17-8 (24%). This inversion suggests that the high accessibility of exchange sites within the macropores, while beneficial for kinetics, simultaneously increases the exposure of the vulnerable quaternary ammonium nitrogen to nucleophilic attack by hydroxide/water species in hot acidic media. The highest loss was observed for the monodisperse gel-type SA6700 (30%), likely due to its specific polymer cross-linking and particle-size uniformity creating high local stress during swelling.

Third, lead retention during cycling requires specific operational attention. As noted in Section 3.6, the incomplete desorption of Pb (68–72%) combined with its slower sorption kinetics suggests gradual Pb accumulation on the sorbent. While the SEC loss remains moderate after three cycles, the accumulation of strongly bound $PbCl_n^{n-}$ complexes may progressively block adjacent exchange sites, potentially accelerating the effective loss of capacity for Zn uptake in long-term industrial cycling.

3.6. Desorption Behavior

To assess the possibility of repeated use of the sorbents, their desorption ability was studied. The degree of desorption of Zn and Pb after three sorption–desorption cycles is given in Table 5.

Table 5. Degree of desorption of Zn and Pb.

Sorbent	AMP-p	AV-17-8	LSC662	LSC688	SA6700 Cl
D(Zn), %	73.0	62.0	55.0	41.0	48.0
D(Pb), %	68.0	30.0	72.0	52.0	44.0

The macroporous pyridinium sorbent AMP-p exhibits the best desorption characteristics among the studied materials; among gel-type sorbents, the differences are less pronounced. This difference may be due to the greater reversibility of the interaction of pyridinium groups with $ZnCl_4^{2-}$: protonation by acid, which effectively competes with zinc for the coordination centers. For the gel-type pyridinium sorbent, the degree of desorption is lower than for the macroporous one, which is due to diffusion limitations in the gel pores rather than to chemical differences in the functional groups.

From a practical standpoint, the use of 10% H_2SO_4 as an eluent is advantageous because it provides a sufficiently high degree of zinc desorption (up to 73% in static tests and 99% in dynamic column tests, Section 4) at a moderate acid concentration, which reduces reagent consumption and simplifies the regeneration scheme compared with ammonia or sodium hydroxide solutions.

At the same time, the desorption of lead is less complete: even for the best sorbents, D(Pb) does not exceed 72% (LSC662) and 68% (AMP-p). This indicates that lead is more strongly retained by the anion exchanger, presumably through stronger binding to the pyridinium groups or through partial incorporation into the matrix, and that more severe desorption conditions (higher acid concentration, elevated temperature, or an additional complexing agent) may be required for its complete removal.

The combination of a lower Pb recovery (Table 2) and a stronger Pb retention (Table 5) reflects two different aspects of the sorption process: the lower R(Pb) values are primarily a kinetic and steric effect (slow diffusion of bulky $PbCl_n^-$ complexes), whereas the stronger retention (lower D(Pb)) is a thermodynamic effect (high polarizability and affinity for the pyridinium ring). This behavior is consistent with the strong affinity of pyridinium groups for $PbCl_n^-$ and with the known difficulty of stripping large, strongly sorbed chloro-complexes from strongly basic anion exchangers; similar incomplete desorption of Zn chloride complexes from strongly basic resins has been reported by Wołowicz [28].

In industrial operation, these two effects act in the same direction during cycling—toward gradual Pb accumulation on the sorbent, which may eventually block exchange sites available for zinc uptake. Therefore, the process design should envisage periodic "hard" regeneration (e.g., higher acid concentration or elevated temperature) to strip the residual Pb, with the Pb balance across the sorption–desorption loop monitored as a routine diagnostic parameter, rather than relying only on Zn breakthrough capacity.

4. Dynamic Tests of the Macroporous Pyridinium Anion Exchanger

The dynamic tests were carried out under conditions close to the industrial process (70 °C, real catholyte composition), which allows the results to be used for preliminary column sizing. Based on the results of the static experiments and the assessment of chemical stability, the macroporous pyridinium anion exchanger was identified as the most promising sorbent for further testing. Its dynamic characteristics were studied in the purification of

chloride nickel solution from Zn and Pb under conditions close to the real technological process. The breakthrough curve for Zn and Pb sorption is shown in Figure 6. The dynamic sorption parameters for Zn and Pb are given in Table 6.

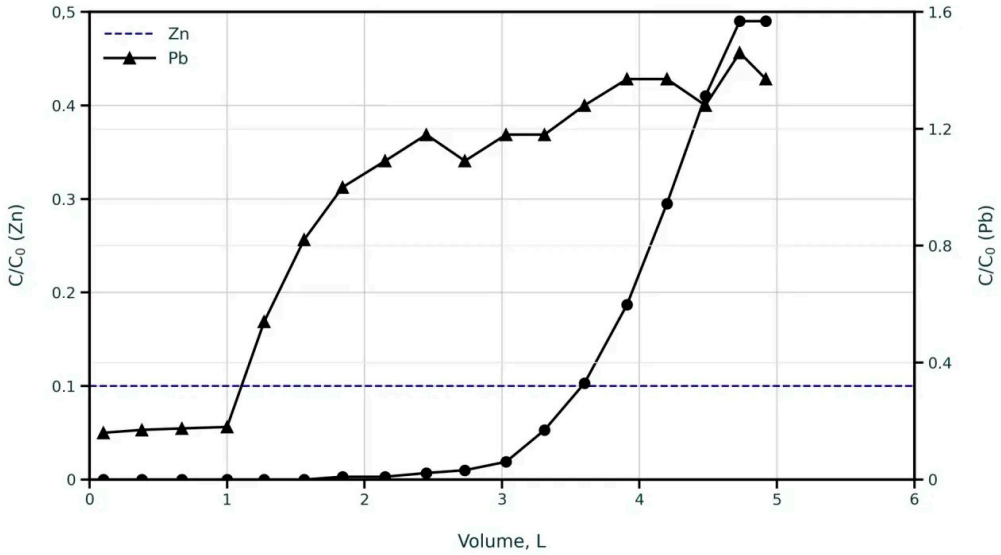


Figure 6. Breakthrough curve for Zn and Pb on the AMP-p sorbent. Conditions: m_{sorb} = 67 g, t = 70 °C, feed rate 5 mL/min.

Table 6. Dynamic sorption parameters for Zn and Pb on AMP-p.

Parameter	Zn	Pb
Sorbent volume, mL	100	100
Sorbent mass (air-dry), g	67	67
Free volume of the column, L	0.038	0.038
Breakthrough volume (10%), L	3.64	1.1
Corrected breakthrough volume, L	3.602	1.062
DBC (at breakthrough point), mmol/g	0.363	$7.57 \cdot 10^{-5}$
Total sorbed metal, mmol	38.26	≈0.020 (curve integration); ≈0.027 (feed-effluent) * *
Total dynamic capacity (TDC), mmol/g	0.571	-
TDC, % of SEC (fresh, 1.19 mmol/g)	48.0	-

* * For Pb, the retained amount was not obtained by integration-based capacity calculation (the Pb loading is close to the analytical detection limit). Two independent estimates are given: integration of the breakthrough curve (≈0.020 mmol) and the feed–effluent difference (≈0.027 mmol, Supplementary Table S2). Note that DBC(Pb) × m = 0.005 mmol represents the amount retained at the breakthrough point (V = 1.1 L) and is consistent with both estimates.

Analysis of the breakthrough curves showed the following. For Zn, the breakthrough curve has a steep front, which is characteristic of processes with favorable kinetics and is due to the macroporous structure of the sorbent: the onset of breakthrough (10% of C_0) was recorded at V_{10}% = 3.64 L, and the run was terminated at V = 5.2 L ($C/C_0 \approx 0.10$); full saturation was not reached within the run. For Pb, breakthrough ($C/C_0 \approx 0.1$) is observed at a much smaller volume ($V_{breakthrough} \approx 1.1$ L), which is due to the low initial lead concentration and its selective uptake. The corresponding DBC(Pb) is very low ($7.57 \cdot 10^{-5}$ mmol/g) because of the low C_0(Pb) = 1.1 mg/L; the total Pb retained

(0.0047 mmol, calculated from the desorption balance; see Table 7) is more representative of the Pb uptake capacity than DBC(Pb).

Table 7. Desorption parameters for Zn and Pb from the macroporous pyridinium anion exchanger.

Parameter	Zn	Pb
Amount of sorbed metal, mmol	38.26	0.0047 *
Amount of desorbed metal, mmol	37.88	0.00325
Degree of desorption, %	99.0	12–16
Maximum concentration in a 75 mL fraction, mg/L	6020	2.4
Concentration factor	12.3	2.2

* For Pb, the desorption efficiency is calculated relative to the retained amount estimated from the breakthrough curve (0.020 mmol) and the feed − effluent difference (0.027 mmol); because of the low Pb concentrations (close to the detection limit), the value should be regarded as semi-quantitative.

Using formula (3), the volume of the real industrial solution that can be purified per 1 g of sorbent to the breakthrough point was recalculated. For DBC = 0.363 mmol/g and C_{real} = 0.62 mg/L = 9.48 × 10^{-3} mmol/L: 1 g of sorbent purifies 38.3 L of solution to the breakthrough point.

For an industrial column loaded with 1 m^3 of sorbent (bulk density ~0.67 g/mL), the volume of solution purified before regeneration will be ~25,655 m^3.

After sorption, the column was washed with distilled water at 70 °C (250 mL, 2.5 bed volumes). The washing criterion was the absence of chloride ions and a Zn concentration < 0.1 mg/L.

Desorption was carried out with 10% H_2SO_4 at 40 °C, a flow rate of 2 mL/min, and an eluent volume of 550 mL (5.5 bed volumes). The desorption parameters for Zn and Pb are given in Table 7.

The degree of Pb desorption in the column test (12–16%) was markedly lower than for Zn (99.0%), and the Pb balance did not close: ≈0.017–0.024 mmol of Pb were not recovered in the desorption eluate and not detected in the washing fraction. Several explanations are plausible. First, the low Pb concentrations (1.1 mg/L in the feed; hundredths of mg/L in the effluent) are close to the analytical detection limit, so the dynamic Pb balance is semi-quantitative. Second, part of the Pb may have remained on the resin as strongly retained complexes. Third, elution with 10% H_2SO_4 may be accompanied by precipitation of sparingly soluble $PbSO_4$: the high sulfate concentration suppresses $PbSO_4$ solubility via the common-ion effect, so a fraction of the released Pb(II) could re-precipitate in the bed or in the eluate and escape solution analysis. This hypothesis, although chemically reasonable, was not directly verified in this work; analysis of the exhausted resin (e.g., after acid digestion) or visual/gravimetric control of the eluate for suspended solids would be required to confirm it. In any case, H_2SO_4 is not an optimal eluent for Pb recovery from the loaded sorbent, and this limitation should be considered when planning the regeneration step.

5. Conclusions

In this work, five strongly basic anion exchangers differing in the type of functional group (pyridinium/quaternary ammonium), matrix structure (gel/macroporous), and exchange capacity were assessed for the purification of chloride nickel solution from Zn(II) and Pb(II). Based on the data obtained, the following conclusions can be drawn:

1. The effect of the functional group on Pb selectivity is best isolated by comparing sorbents with the same matrix: AMP-p (pyridinium, macroporous) gives R(Pb) = 62.0% (β = 0.76), whereas LSC688 (quaternary ammonium, macroporous) gives R(Pb)

= 26.7% (β = 0.31). The gel-type pyridinium resin LSC662 gives only R(Pb) = 24.9% (β = 0.29), lower than all quaternary ammonium resins (β = 0.31–0.43): the matrix must be accessible for the pyridinium group to express its affinity for the bulky Pb chloro-complexes, whereas for the smaller Zn chloro-complexes the matrix structure is not limiting (R(Zn) = 80–86% for all sorbents).

2. The macroporous structure substantially improves the kinetics: AMP-p achieves 83.7% Zn removal within 15 min, whereas gel-type sorbents require 60–120 min. Under static single-contact conditions, the exchange capacity is not the limiting factor, and the macroporous sorbent additionally shows the highest tolerance to S:L variation (83.5–92.6% over the 1:10–1:100 range).
3. The advantage of macroporous resins in chemical stability is conditional and depends on the functional group: LSC688 (macroporous, quaternary ammonium) lost 27% of the FTIR signal, more than the gel-type AV-17-8 (24%), so macroporosity alone does not guarantee higher stability. After three sorption-desorption cycles, the SEC losses (17.2–23.1%) were systematically lower than the FTIR losses of functional groups (22–30%), the difference being 4.7–7.9%, which indicates partial preservation of the exchange sites. The absence of a C=O band (1720 cm^{-1}) shows that oxidation via carbonyl-containing products is not the dominant pathway; however, the FTIR data alone cannot distinguish between acid-catalyzed hydrolysis and oxidation, and the degradation mechanism is presented as a hypothesis.
4. Dynamic tests of AMP-p at 70 °C confirmed its efficiency: DBC(Zn) = 0.363 mmol/g (V_{bt} = 3.64 L) and DBC(Pb) = $7.57 \cdot 10^{-5}$ mmol/g (V_{bt} = 1.1 L), with TDC(Zn) = 0.571 mmol/g obtained by integration of the breakthrough curve up to the end of the run. Desorption with 10% H_2SO_4 was nearly complete for Zn (99.0%) and incomplete for Pb (12–16% of the retained Pb (0.020–0.027 mmol, estimated independently from the breakthrough curve and the feed–effluent difference); the unrecovered Pb was not detected in any analyzed solution). Because the Pb concentration in the feed (1.1 mg/L) is close to the detection limit, the dynamic Pb balance should be regarded as semi-quantitative. Recalculation to the real industrial solution (C_0(Zn) = 0.62 mg/L) showed that 1 g of sorbent purifies 38.3 L of solution to the Zn breakthrough point, which corresponds to ≈25,655 m^3 for a column with 1 m^3 of sorbent; since Pb breaks through considerably earlier than Zn, the actual cycle length may be limited by the Pb behaviour and should be verified at realistic Pb concentrations.
5. Based on the combination of functional stability, kinetics, selectivity, and dynamic characteristics, the macroporous pyridinium anion exchanger AMP-p is recommended for the purification of chloride nickel solutions from Zn(II) and Pb(II): it provides the highest Pb uptake among the studied sorbents (R(Pb) = 62.0%) and the best desorption characteristics (Table 5). Its use allows the contact time to be reduced to 15–30 min and operation without cooling the solution (60–70 °C). The preliminary column sizing based on the dynamic data (point 4) indicates the potential for industrial-scale implementation, provided that a Pb management strategy—periodic "hard" regeneration and Pb balance monitoring—is included in the process design.

Further studies should address (i) the long-term performance of the macroporous pyridinium sorbent over a larger number of real-solution cycles; (ii) the fate of the unrecovered Pb, in particular by analysis of the exhausted resin (e.g., after acid digestion) and by control of the desorption eluate for suspended solids; and (iii) the Pb behaviour at realistic feed concentrations, which may require more severe desorption conditions than zinc. The lower Pb recovery combined with its stronger retention indicates that lead may gradually accumulate on the sorbent during extended industrial cycling; therefore, periodic "hard" regeneration (higher acid concentration, elevated temperature, or an additional complexing

agent) or periodic sorbent replacement should be envisaged, and the Pb balance across the sorption–desorption loop should be monitored as a routine diagnostic parameter.

Supplementary Materials: The following supporting information can be downloaded at https://www.mdpi.com/article/10.3390/met16121305/s1. Table S1. Breakthrough curve data for Zn and Pb on AMP-p and calculation of dynamic capacities. Part A: calculation of DBC and TDC by trapezoidal integration of the breakthrough curve; Part B: breakthrough curve points (V, C/C_0) for Zn and Pb; Table S2. Material balance for Zn and Pb in the dynamic column test on AMP-p. Part A: feed and effluent; Part B: washing; Part C: desorption; Part D: closure of the balance.

Author Contributions: Conceptualization, E.B., N.T. and A.K.; methodology, E.B. and N.T.; software, E.B.; formal analysis, E.B., N.T. and A.K.; investigation, E.B.; resources, N.T.; data curation, N.T.; writing—original draft preparation, E.B.; writing—review and editing, E.B., N.T. and A.K.; visualization, E.B.; project administration, E.B., N.T. and A.K.; funding acquisition, E.B. and N.T. All authors have read and agreed to the published version of the manuscript.

Funding: This study is supported by the Ministry of Science and Higher Education of the Russian Federation; scientific topic No. FMEZ-2025-0059 (registration 1023032400207-6).

Data Availability Statement: The original contributions presented in this study are included in the article and Supplementary Material. Further inquiries can be directed to the corresponding author.

Conflicts of Interest: Author Elena Belogurova was employed by the company Joint-Stock Company "Group of Companies "Rusredmet". The remaining authors declare that the research was conducted in the absence of any commercial or financial relationships that could be construed as a potential conflict of interest.

References

1. Kononova, O.N.; Mikhaylova, N.V.; Melnikov, A.M.; Kononov, Y.S. Ion exchange recovery of zinc from chloride and chloride-sulfate solutions. *Desalination* **2011**, *274*, 150–155. [CrossRef]
2. Zhang, G.-Q.; Zhang, Q.-X.; Xiao, L.-S.; Gong, B.-F. Study on removing zinc from nickel electrolyte by ion-exchange. *J. Cent. South. Univ.* **2000**, *7*, 194–197. [CrossRef]
3. Kasikov, A.G.; Dyakova, L.V.; Sokolov, A.Y. Purification of concentrated nickel chloride-sulfate solutions of «Kola MMC» JSC from impurities by solvent extraction. *Chem. Eng.* **2023**, *24*, 463–469. [CrossRef]
4. Meyer, G.A.; Peters, M.A.; Leaver, H.S. Purification of Nickel Chloride Solutions. U.S. Patent US4221765A, 9 September 1980.
5. Aprahamian, V.H.; Demopoulos, G.P. The Solution Chemistry and Solvent Extraction Behaviour of Cu, Fe, Ni, Zn, Pb, Sn, Ag, As, Sb, Bi, Se and Te in Acid Chloride Solutions Reviewed from the Standpoint of PGM Refining. *Miner. Process. Extr. Metall. Rev.* **1995**, *14*, 143–167. [CrossRef]
6. Jha, M.K.; Kumar, V.; Singh, R.J. Solvent Extraction of Zinc from Chloride Solutions. *Solvent Extr. Ion. Exch.* **2002**, *20*, 389–405. [CrossRef]
7. Najafi, F.; Dolatyari, L.; Shayani-Jam, H.; Yaftian, M.R. Aliquat IL336 vs. Cyphos IL101 extractants for the solvent extraction of heavy metals from zinc plants residues. *Sci. Rep.* **2026**, *16*, 25821. [CrossRef]
8. Sarfraz, S.; Ahmad, M.; Barri, A.; Ali, A.; Luqman, M.; Ul Islam, G.; Amin, S.; Qayyum, M.A.; Al-Ahmary, K.M.; Ahmed, M.; et al. Applicability of supported liquid membranes for extraction of Zn^{2+} and Ni^{2+} in water using cyclohexylamine as a carrier. *J. Chem.* **2025**, *2025*, 1743726. [CrossRef]
9. Mekahlia, S. Le Complexe Chitosane-Cuivre (II): Synthèse, Caractérisation et étude de l'effet de sa Structure sur son Activité Antibactérienne. Master's Thesis, Université Saad Dahlab de Blida, Blida, Algeria, 2007.
10. Chugunov, A.D. Physico-Chemical Features of Adsorption of Heavy Metal Ions by Zeolites Modified with Organosilicon Thiosemicarbazides. Ph.D. Dissertation, Irkutsk National Research Technical University, Irkutsk, Russia, 2024.
11. BenchChem Technical Support Team. Preventing Metal Ion Leakage from Iminodiacetate Resins. BenchChem Technical Documentation, April 2026. Available online: https://pdf.benchchem.com/1231/Preventing_metal_ion_leakage_from_Iminodiacetate_resins.pdf (accessed on 20 October 2026).
12. Cheng, S.; Ma, Y.; Zhang, J.; Xi, H.; Sun, Y.; Zong, H.; Guo, Y.; Li, Y. Preparation of ionic liquid composite resin and its application in removing zinc from nickel electrolyte. *Nonferrous Met.* **2024**, *14*, 41–48. [CrossRef]
13. Chen, Z.; Tan, D.S.; Li, Q.W.; Shao, Q.Y.; Wang, J.J.; Zhang, L.F.; Xie, J.Y.; Zou, X.J. Thermodynamics and kinetics of adsorption of Zn(II) from chloride solution using DOWEX MSA-1 anion exchange resin. *Hydrometall. China* **2023**, *42*, 30–36. [CrossRef]

14. Barlık, N. Sorption of zinc chloride complexes from acid-based solutions by using anionic resins: Process optimization and modeling. *Int. J. Environ. Sci. Technol.* **2024**, *21*, 8959–8975. [CrossRef]
15. Chen, S.; Guo, X.; Li, J.; Tian, Q.; Liang, S. Behavior and removal methods of lead and zinc in the nickel electrolyte. *Nonferrous Met. (Extr. Metall.)* **2008**, *6*, 6–8. (In Chinese)
16. Zhu, A. Research status on purification methods of nickel solution. *Hydrometall. China* **2012**, *31*, 71–75. (In Chinese) [CrossRef]
17. Kaur, G.; Couperthwaite, S.J.; Millar, G.J. Ion exchange processes for the recovery of metals from hydrometallurgical streams: A review. *Hydrometallurgy* **2020**, *191*, 105–216.
18. Alexandratos, S.D. Ion-exchange resins: A retrospective from industrial and engineering chemistry research. *Ind. Eng. Chem. Res.* **2009**, *48*, 388–398. [CrossRef]
19. Areshina, N.S.; Kasikov, A.G.; Timoshchik, O.A.; Shevtsov, A.V. Application of the sorption method in the schemes for purifying nickel solutions of JSC "Kola MMC" from zinc. *Tr. Kol'skogo Nauchnogo Tsentra RAN. Seriya Tekhnicheskie Nauk.* **2025**, *16*, 149–153. [CrossRef]
20. Imamura, M. Purification Method of Nickel Chloride Solution. Japanese Patent JP2003147452A, 21 May 2003.
21. Kołodyńska, D.; Hubicka, H.; Hubicki, Z. Sorption of heavy metal ions from aqueous solutions in the presence of EDTA on monodisperse anion exchangers. *Desalination* **2008**, *227*, 150–166. [CrossRef]
22. Neagu, V.; Bunia, I.; Plesca, I. Ionic polymers VI. Chemical stability of strong base anion exchangers in aggressive media. *Polym. Degrad. Stab.* **2000**, *70*, 463–468. [CrossRef]
23. Nishikawa, I.; Takaishi, K.; Matsumoto, N. Purification Method of Nickel Chloride Aqueous Solution. Japanese Patent JP2005247666A, 15 September 2005.
24. Helfferich, F. *Ion Exchange*; McGraw-Hill: Dover, UK, 1995.
25. Zagorodni, A.A.; Kotova, D.L.; Selemenev, V.F. Infrared spectroscopy of ion exchange resins: Chemical deterioration of the resins. *React. Funct. Polym.* **2002**, *53*, 157–171. [CrossRef]
26. Gutsanu, V.; Tudorachi, N.; Lisa, G. The behavior of the AV-17(Cr) sorbent in various media. *Thermochim. Acta* **2013**, *560*, 109–115. [CrossRef]
27. *DIN 54402:2009-04*; Testing of Ion Exchangers—Determination of the Total Capacity of Anion Exchangers. Beuth Verlag: Berlin, Germany, 2009.
28. Wołowicz, A. Zinc(II) removal from model chloride and chloride–nitrate(V) solutions using various sorbents. *Physicochem. Probl. Miner. Process.* **2019**, *55*, 1517–1534. [CrossRef]

Disclaimer/Publisher's Note: The statements, opinions and data contained in all publications are solely those of the individual author(s) and contributor(s) and not of MDPI and/or the editor(s). MDPI and/or the editor(s) disclaim responsibility for any injury to people or property resulting from any ideas, methods, instructions or products referred to in the content.